

Fast communication

# Improved MUSIC algorithm for high resolution angle estimation

Wei-ke Nie<sup>a,\*</sup>, Da-zheng Feng<sup>b</sup>, Hu Xie<sup>b</sup>, Jin Li<sup>b</sup>, Peng-fei Xu<sup>a</sup><sup>a</sup> School of Information Science and Technology, Northwest University, Xi'an 710127, China<sup>b</sup> National Lab of Radar Signal Processing, Xidian University, Xi'an 710071, China

## ARTICLE INFO

## Article history:

Received 20 July 2015

Received in revised form

12 November 2015

Accepted 7 December 2015

Available online 14 December 2015

## keywords:

Array antennas

MUSIC algorithm

Signal subspace

## ABSTRACT

By using a single correlation matrix, classic MUSIC algorithm estimates subspaces through traditional eigenvalue decomposition. Its performances suffered from these inaccurate subspaces greatly. In this paper, a set of spatial temporal correlation matrices are firstly constructed by exploiting the array received data. Secondly, in order to get more accurate subspace, we establish a uniform cost function that exploits these matrices. Thirdly, a cyclic optimization algorithm is designed to jointly estimate the signal subspace. Moreover, by the relation between signal and noise subspace, the corresponding projection matrix of noise subspace is obtained, hence an improved MUSIC algorithm is implemented by this projection matrix. Finally three experiments are conducted to validate the performances of the proposed algorithm.

© 2015 Elsevier B.V. All rights reserved.

## 1. Introduction

Multiple Signal Classification (MUSIC) algorithm [1] is a well-known high resolution direction of arrival (DOA) estimation method. Its performances mainly depend on the accuracy of estimated subspace [2]. However, the subspace in classic MUSIC is obtained by the traditional eigenvalue decomposition of the single zero delay correlation matrix. Such a subspace will dramatically decline [3] the performances of MUSIC in some cases. One is the signal to noise ratio (SNR) lower than 0 dB, which makes the signal and noise subspace be difficultly distinguished. Therefore, an incorrect subspace is obtained. Another case is in small snapshots, an imprecise correlation matrix is derived, and its eigvalue decomposition estimates a coarse subspace. Both critically limit the performances [4] of MUSIC algorithm.

This paper sufficiently utilizes the spatial temporal domain information. By exploiting two subarrays and their multiple delay received data, a set of spatial temporal correlation matrices are constructed. These matrices are written into a uniform expression for establishing a cost function. A novel cyclic optimization algorithm is proposed to jointly estimate the signal subspace. Then the projection matrix of noise subspace is obtained, from which the improved MUSIC algorithm is proposed. All these are the main contributions of this paper.

In the simulations, the accuracy of estimated subspace by the proposed cyclic optimization is compared with the traditional eigenvalue decomposition. Then the spatial spectrums of the improved MUSIC and the classical MUSIC are also simulated to demonstrate the improvement of the resolution. The root mean square error (RMSE) of estimated angle is also presented. Each of the performance is analyzed versus SNR, snapshots and the number of sensors. Simulations show that the proposed algorithm possesses better performances than classic MUSIC algorithm in the same scenarios.

\* Corresponding author. Tel.: +86 13891933536.  
E-mail address: [weikenie@163.com](mailto:weikenie@163.com) (W.-k. Nie).

## 2. Problem formulation

Consider a uniform linear array (ULA) composed of  $M$  ( $m = 1, 2, \dots, M$ ) sensors on which  $P$  narrow band non-coherent far field signals are impinging with different DOAs. The signal arriving at the  $m$ th sensor is

$$x_m(t) = \sum_{p=1}^P a_{mp} s_p(t) + n_m(t) \quad (1)$$

where  $a_{mp} = \exp[j(2\pi/\lambda)(m-1)d \sin \theta_p]$ ,  $d$  is the spacing between adjacent sensor elements,  $\lambda$  is the wavelength and  $\theta_p$  is the DOA relative to the array broadside. The array output at  $t$ th snapshot can be expressed as

$$\mathbf{x}(t) = [x_1(t), x_2(t), \dots, x_M(t)]^T = \mathbf{A}\mathbf{s}(t) + \mathbf{n}(t) \quad (2)$$

where  $T$  represents the transpose,  $\mathbf{A} = [\mathbf{a}_1, \mathbf{a}_2, \dots, \mathbf{a}_P]$  is the array direction matrix,  $\mathbf{a}_p = [a_{1p}, a_{2p}, \dots, a_{Mp}]^T$  is the steering vector ( $p = 1, 2, \dots, P$ ),  $\mathbf{s}(t) = [s_1(t), s_2(t), \dots, s_P(t)]^T$  is the vector of source waveforms. Noise vector  $\mathbf{n}(t) = [n_1(t), n_2(t), \dots, n_M(t)]^T$  is assumed to be zero-mean and independent of the observed signal. The zero delay correlation matrix of the received data is defined as

$$\mathbf{R}_x(0) = E[\mathbf{x}(t)\mathbf{x}^H(t)] = \mathbf{A}\mathbf{R}_s(0)\mathbf{A}^H + \sigma^2\mathbf{I} \quad (3)$$

where  $\sigma^2$  and  $\mathbf{I}$  represent noise power and unit matrix,  $H$  represents the complex conjugate transpose. The eigenvalue decomposition of  $\mathbf{R}_x(0)$  can be written as

$$\mathbf{R}_x(0) = \mathbf{U}_s \mathbf{\Lambda}_s \mathbf{U}_s^H + \sigma^2 \mathbf{U}_n \mathbf{U}_n^H \quad (4)$$

where  $\mathbf{\Lambda}_s$  is diagonal matrix with signal eigenvalues,  $\mathbf{U}_s$  and  $\mathbf{U}_n$  are signal and noise subspaces respectively. The MUSIC algorithm computes [1,5] the spatial spectrum by

$$P_{MUSIC}(\hat{\theta}) = \frac{1}{|\mathbf{a}^H(\hat{\theta})\mathbf{U}_n\mathbf{U}_n^H\mathbf{a}(\hat{\theta})|} \quad (5)$$

where  $\mathbf{a}(\hat{\theta})$  is the steering vector. It is well-known that when signal or noise subspace is accurate enough obtained and  $\hat{\theta}$  equals to the actual DOA, the spatial spectrum will show a peak.

## 3. Improved MUSIC algorithm

In the proposed algorithm, we separate the above mentioned ULA into two subarrays. Let the first and second subarrays be composed of the sensors with the indices  $1, 2, \dots, M-1$  and  $2, 3, \dots, M$ , respectively. The received signal vector of the first and second subarray can be written as

$$\mathbf{x}_1(t) = \mathbf{A}_1(\theta)\mathbf{s}(t) + \mathbf{n}_1(t) \quad (6)$$

$$\mathbf{x}_2(t) = \mathbf{A}_2(\theta)\mathbf{s}(t) + \mathbf{n}_2(t) = \mathbf{A}_1(\theta)\Phi\mathbf{s}(t) + \mathbf{n}_2(t) \quad (7)$$

where  $\mathbf{A}_2 = \mathbf{A}_1\Phi$ ,  $\Phi = \text{diag}[\exp(j\omega_1), \exp(j\omega_2), \dots, \exp(j\omega_P)]$ ,  $\omega_p = 2\pi d(\sin \theta_p)/\lambda$ . Let  $\mathbf{R}_s(k)$  represent the sample correlation matrix of the source signal vector which is given by

$$E[\mathbf{s}(t)\mathbf{s}(t+k)^H] = \mathbf{R}_s(k) \quad (8)$$

Let  $\mathbf{R}_{m,n}(k)$  ( $m, n = 1, 2$ ) represent the spatio temporal correlation matrices between the  $m$ th subarray and the

$n$ th subarray. We have the following equations:

$$\mathbf{R}_{1,1}(k) = \mathbf{A}_1\mathbf{R}_s(k)\mathbf{A}_1^H \quad (9a)$$

$$\mathbf{R}_{1,2}(k) = \mathbf{A}_1\mathbf{R}_s(k)\mathbf{A}_2^H = \mathbf{A}_1\mathbf{R}_s(k)\Phi^H\mathbf{A}_1^H \quad (9b)$$

$$\mathbf{R}_{2,1}(k) = \mathbf{A}_2\mathbf{R}_s(k)\mathbf{A}_1^H = \mathbf{A}_1\Phi\mathbf{R}_s(k)\mathbf{A}_1^H \quad (9c)$$

$$\mathbf{R}_{2,2}(k) = \mathbf{A}_2\mathbf{R}_s(k)\mathbf{A}_2^H = \mathbf{A}_1\Phi\mathbf{R}_s(k)\Phi^H\mathbf{A}_1^H \quad (9d)$$

Eqs. (9a)–(9d) can be written in a uniform expression as

$$\mathbf{R}_{m,n}(k) = \mathbf{A}_1\mathbf{\Lambda}_m[\mathbf{B}_n(k)]^H \quad (m, n = 1, 2; k = 0, 1, \dots, K) \quad (10)$$

where  $\mathbf{\Lambda}_m = \Phi^{m-1}$  ( $m = 1, 2$ ) are diagonal matrices,  $\mathbf{B}_n(k) = \mathbf{A}_n\mathbf{R}_s^H(k)$  ( $n = 1, 2$  and  $k = 0, 1, \dots, K$ ). In order to fully exploit the information in the set of matrices expressed in (10) and jointly estimate the signal subspace, we construct the following uniform cost function:

$$\max J(\mathbf{U}, \mathbf{V}) = \sum_{k=1}^K \sum_{n=1}^2 \sum_{m=1}^2 \|\mathbf{U}^H \mathbf{R}_{m,n}(k) \mathbf{V}\|_F^2 \quad (11a)$$

$$\text{s. t. } \mathbf{U}^H \mathbf{U} = \mathbf{I}, \quad \mathbf{V}^H \mathbf{V} = \mathbf{I} \quad (11b)$$

where subscript  $F$  denotes the Frobenius matrix. If we fix  $\mathbf{U}$  as  $\underline{\mathbf{U}}$ , the cost function can be rewritten as

$$\begin{aligned} \max J(\underline{\mathbf{U}}, \mathbf{V}) &= \sum_{k=1}^K \sum_{n=1}^2 \sum_{m=1}^2 \|\underline{\mathbf{U}}^H \mathbf{R}_{m,n}(k) \mathbf{V}\|_F^2 \\ &= \sum_{k=1}^K \sum_{n=1}^2 \sum_{m=1}^2 \text{tr}\{[\mathbf{V}^H \mathbf{R}_{m,n}^H(k) \underline{\mathbf{U}} \underline{\mathbf{U}}^H \mathbf{R}_{m,n}(k) \mathbf{V}]\} \end{aligned} \quad (12a)$$

$$\text{s. t. } \mathbf{V}^H \mathbf{V} = \mathbf{I} \quad (12b)$$

where  $\text{tr}(\bullet)$  indicates a matrix trace. By using Lagrange multiplier method and matrix differential calculus [6], the optimization problem can be converted into an unconstrained one

$$\begin{aligned} \max J(\underline{\mathbf{U}}, \mathbf{V}, \tilde{\mathbf{\Lambda}}_1) &= \sum_{k=1}^K \sum_{n=1}^2 \sum_{m=1}^2 \text{tr} \\ &\quad \{[\mathbf{V}^H \mathbf{R}_{m,n}^H(k) \underline{\mathbf{U}} \underline{\mathbf{U}}^H \mathbf{R}_{m,n}(k) \mathbf{V}]\} \\ &\quad - \text{tr}[(\mathbf{V}^H \mathbf{V} - \mathbf{I}) \tilde{\mathbf{\Lambda}}_1] \end{aligned} \quad (13)$$

where  $\tilde{\mathbf{\Lambda}}_1$  are Lagrange multiplier matrix, letting the gradient of  $J(\underline{\mathbf{U}}, \mathbf{V}, \tilde{\mathbf{\Lambda}}_1)$  with respect to  $\mathbf{V}$  be equal to zero, we have

$$\left\{ \sum_{k=1}^K \sum_{n=1}^2 \sum_{m=1}^2 [\mathbf{R}_{m,n}^H(k) \underline{\mathbf{U}} \underline{\mathbf{U}}^H \mathbf{R}_{m,n}(k)] \right\} \mathbf{V} - \mathbf{V} \tilde{\mathbf{\Lambda}}_1 = \mathbf{0} \quad (14)$$

Solving (14) can get the signal subspace. However, it is difficult to solve the nonlinear Eq. (14). If the matrix in big bracket of (14) is not changed with  $\mathbf{U}$ , then expression

(14) describes a standard eigen decomposition of  $\sum_{k=1}^K$

$\sum_{n=1}^2 \sum_{m=1}^2 [\mathbf{R}_{m,n}^H(k) \underline{\mathbf{U}} \underline{\mathbf{U}}^H \mathbf{R}_{m,n}(k)]$ . Similarly, if we fix  $\mathbf{V}$  as  $\underline{\mathbf{V}}$ , the

cost function (11) takes the following form:

$$\max J(\mathbf{U}, \underline{\mathbf{V}}) = \sum_{k=1}^K \sum_{n=1}^2 \sum_{m=1}^2 \|\mathbf{U}^H \mathbf{R}_{m,n}(k) \underline{\mathbf{V}}\|_F^2$$

$$= \sum_{k=1}^K \sum_{n=1}^2 \sum_{m=1}^2 \text{tr} \{ [\mathbf{U}^H \mathbf{R}_{m,n}(k) \mathbf{V}] [\mathbf{V}^H \mathbf{R}_{m,n}^H(k) \mathbf{U}] \} \quad (15a)$$

$$\text{s. t. } \mathbf{U}^H \mathbf{U} = \mathbf{I} \quad (15b)$$

as mentioned above, the optimization problem can be converted into an unconstrained one

$$\begin{aligned} \max J(\mathbf{U}, \mathbf{V}, \hat{\Lambda}_2) = & \sum_{k=1}^K \sum_{n=1}^2 \sum_{m=1}^2 \text{tr} \\ & \{ [\mathbf{U}^H \mathbf{R}_{m,n}(k) \mathbf{V}] [\mathbf{V}^H \mathbf{R}_{m,n}^H(k) \mathbf{U}] \} \\ & - \text{tr}[(\mathbf{U}^H \mathbf{U} - \mathbf{I}) \hat{\Lambda}_2] \end{aligned} \quad (16)$$

where  $\hat{\Lambda}_2$  are Lagrange multiplier matrix, Letting the gradient of  $J(\mathbf{U}, \mathbf{V}, \hat{\Lambda}_2)$  with respect to  $\mathbf{U}$  be equal to zero, we have

$$\left\{ \sum_{k=1}^K \sum_{n=1}^2 \sum_{m=1}^2 [\mathbf{R}_{m,n}(k) \mathbf{V} \mathbf{V}^H \mathbf{R}_{m,n}^H(k)] \right\} \mathbf{U} - \mathbf{U} \hat{\Lambda}_2 = \mathbf{0} \quad (17)$$

it describes a standard eigen decomposition of  $\sum_{k=1}^K \sum_{n=1}^2 \sum_{m=1}^2 [\mathbf{R}_{m,n}(k) \mathbf{V} \mathbf{V}^H \mathbf{R}_{m,n}^H(k)]$ . The above derivation makes us to propose a cyclic optimization algorithm to jointly derive the signal subspace. This cyclic optimization algorithm uses repeatedly the eigen decomposition and can be described as follows. Produce randomly the initial values as  $\mathbf{U}(0) = [\mathbf{u}_1(0) \ \mathbf{u}_2(0) \ \dots \ \mathbf{u}_P(0)]$  with dimension  $(M-1) \times P$ , without loss of generality, in the  $l$ th  $l = 1, 2, \dots, L$  circulation, let

$$\tilde{\mathbf{C}} = \sum_{k=1}^K \sum_{n=1}^2 \sum_{m=1}^2 [\mathbf{R}_{m,n}^H(k) \mathbf{U}(l-1) \mathbf{U}^H(l-1) \mathbf{R}_{m,n}(k)] \quad (18)$$

let the eigen decomposition of  $\tilde{\mathbf{C}}$  is  $\tilde{\mathbf{C}}_{\text{eig}}$

$$\tilde{\mathbf{C}}_{\text{eig}} = \bar{\mathbf{V}}(l-1) \bar{\mathbf{D}}(l-1) \bar{\mathbf{V}}^H(l-1) \quad (19)$$

where  $\bar{\mathbf{D}}(l-1) = \text{diag}[\bar{d}_1(l-1), \bar{d}_2(l-1), \dots, \bar{d}_{M-1}(l-1)]$  is the diagonal eigenvalue matrix with  $\bar{d}_1(l-1) \geq \bar{d}_2(l-1) \geq \dots \geq \bar{d}_{M-1}(l-1) \geq 0$ ,  $\bar{\mathbf{V}}(l-1)$  is the eigenvector matrix of  $\tilde{\mathbf{C}}$ . Let matrix  $\mathbf{V}(l-1)$  be constructed by the first  $P$  columns [7,8] of  $\bar{\mathbf{V}}(l-1)$ , then let

$$\hat{\mathbf{C}} = \sum_{k=1}^K \sum_{n=1}^2 \sum_{m=1}^2 [\mathbf{R}_{m,n}(k) \mathbf{V}(l-1) \mathbf{V}^H(l-1) \mathbf{R}_{m,n}^H(k)] \quad (20)$$

let the eigen decomposition of  $\hat{\mathbf{C}}$  is  $\hat{\mathbf{C}}_{\text{eig}}$

$$\hat{\mathbf{C}}_{\text{eig}} = \hat{\mathbf{U}}(l) \hat{\mathbf{D}}(l) \hat{\mathbf{U}}^H(l) \quad (21)$$

where  $\hat{\mathbf{D}}(l) = \text{diag}[\hat{d}_1(l), \hat{d}_2(l), \dots, \hat{d}_{M-1}(l)]$  is the diagonal eigenvalue matrix with  $\hat{d}_1(l) \geq \hat{d}_2(l) \geq \dots \geq \hat{d}_{M-1}(l) \geq 0$ ,  $\hat{\mathbf{U}}(l)$  is the eigenvector matrix of  $\hat{\mathbf{C}}$ , let matrix  $\mathbf{U}(l)$  be constructed by the first  $P$  column of  $\hat{\mathbf{U}}(l)$ . Until now we give one circulation from  $\mathbf{U}(l-1)$  to  $\mathbf{U}(l)$ , the remaining work is the substitution of  $\mathbf{U}(l)$  in Eq. (18) and perform another circulation. We can circularly optimize  $\mathbf{U}(l)$  until convergence, suppose the threshold is  $\varepsilon$  ( $0 < \varepsilon < 1$ ), if  $\|\mathbf{U}(l) \mathbf{U}^H(l) - \mathbf{U}(l-1) \mathbf{U}^H(l-1)\|_F < \varepsilon$ , then the circulation is stopped and the proposed signal subspace is marked as  $\hat{\mathbf{U}}_s = \mathbf{U}(l)$ . According to the relation [9] of signal and noise subspace, we can get the projection matrix of noise

subspace as

$$\hat{\mathbf{U}}_n \hat{\mathbf{U}}_n^H = \mathbf{I} - \hat{\mathbf{U}}_s \hat{\mathbf{U}}_s^H \quad (22)$$

Hence, the spatial spectrum of the improved MUSIC algorithm can be given as

$$P_{\text{proposed}}(\hat{\theta}) = \frac{1}{|\mathbf{a}^H(\hat{\theta})(\mathbf{I} - \hat{\mathbf{U}}_s \hat{\mathbf{U}}_s^H) \mathbf{a}(\hat{\theta})|} \quad (23)$$

## 4. Simulation results

In this section, simulations are presented to illustrate the performances of the improved MUSIC algorithm. A uniform linear array is used and two narrow band non-coherent far field signals come from  $\theta_1 = -3^\circ$  and  $\theta_2 = 3^\circ$ .  $K$  in Eq. (10) is set to be 4, i.e. 20 spatial temporal correlation matrices are constructed. Except the performance simulations versus sensor number, we fixed the sensor number in other experiments to be 13. Experiments 1 and 2 have been averaged over 100 Monte Carlo runs. And experiment 3, 1000 Monte Carlo runs.

### 4.1. Experiment 1: subspace accuracy of the proposed and MUSIC algorithm

The theoretical signal subspace is  $\mathbf{U}_s = \mathbf{A}_1(\mathbf{A}_1^H \mathbf{A}_1)^{-\frac{1}{2}}$ , the projection matrix of  $\mathbf{U}_s$  is  $\mathbf{P}_s = \mathbf{U}_s \mathbf{U}_s^H$ , and the projection matrix of estimated signal subspace is  $\hat{\mathbf{P}}_s = \hat{\mathbf{U}}_s \hat{\mathbf{U}}_s^H$ . Let  $\hat{\mathbf{P}}_{sn}$  represent the projection matrix of the  $n$ th independent estimation of signal subspace, the accuracy of signal subspace can be defined as  $10 \log_{10}(\frac{1}{N} \sum_{n=1}^N \|\mathbf{P}_{sn} - \hat{\mathbf{P}}_{sn}\|_F)$ .

Fig. 1 shows the accuracy of signal subspace versus SNR. The figure demonstrates that the proposed algorithm possesses better signal subspace accuracy than classic MUSIC, and increases the accuracy about 5 dB when the snapshots at 200 and 500. Fig. 2 shows the accuracy of signal subspace versus snapshots. The figure demonstrates that the proposed algorithm possesses better signal

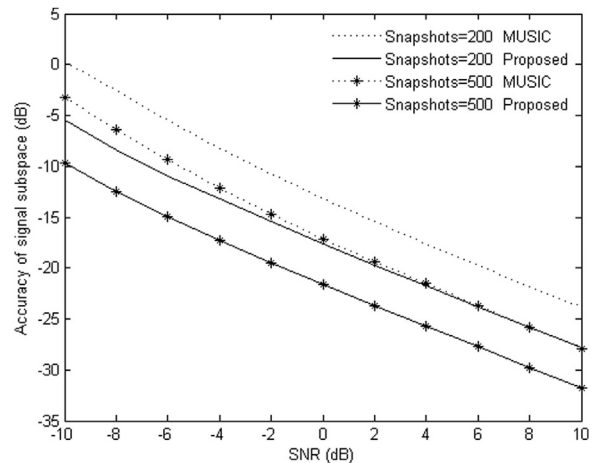


Fig. 1. Accuracy of signal subspace versus SNR.

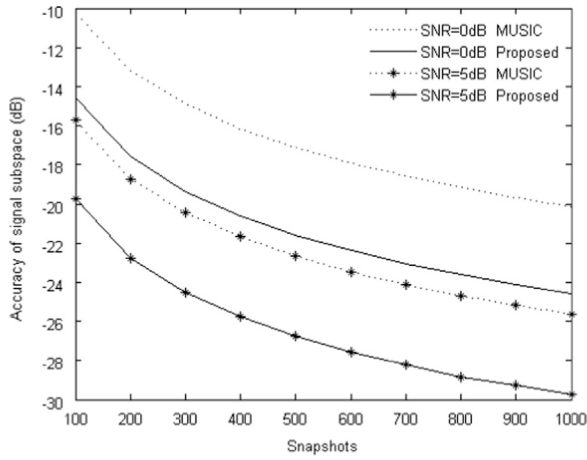


Fig. 2. Accuracy of signal subspace versus snapshots.

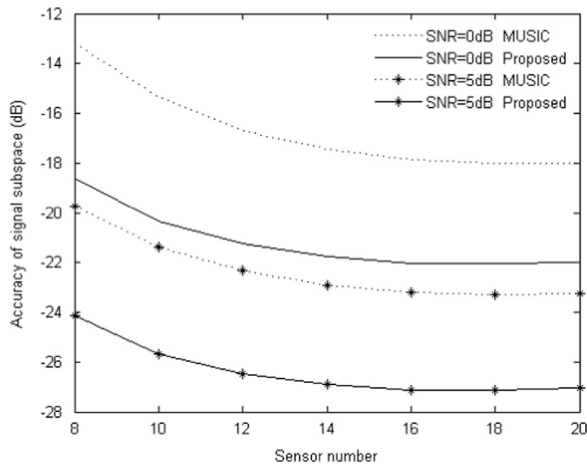


Fig. 3. Accuracy of signal subspace versus sensor number.

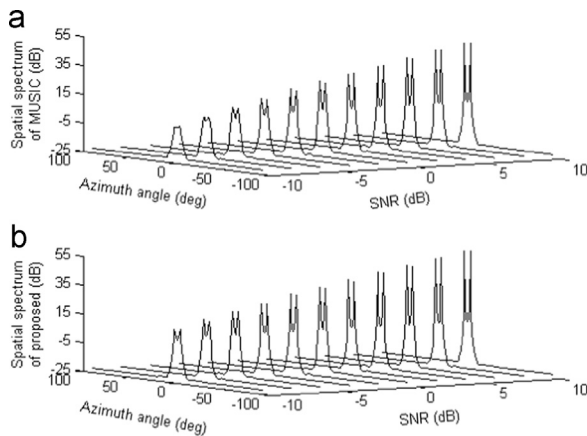


Fig. 4. Spatial spectrum versus SNR.

subspace accuracy than classic MUSIC, and can increase the accuracy about 5 dB when the SNR at 0 dB and 5 dB. Fig. 3 shows the accuracy of signal subspace versus sensor number, where the snapshots is set to be 500. The figure demonstrates that the proposed algorithm possesses

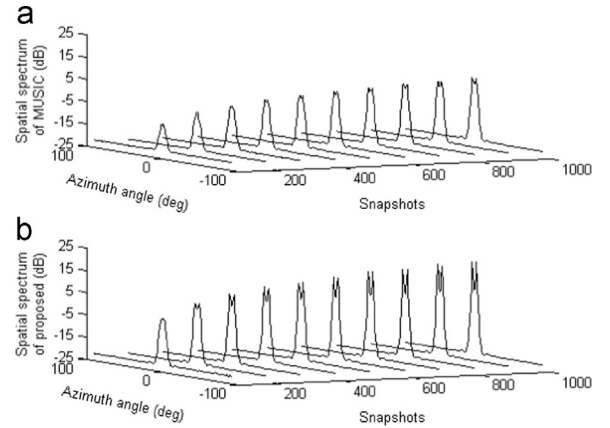


Fig. 5. Spatial spectrum versus snapshots.

better signal subspace accuracy than classic MUSIC, and can increase the accuracy about 4 dB when the SNR at 0 dB and 5 dB.

#### 4.2. Experiment 2: spatial spectrum comparisons of the proposed and MUSIC algorithm

Fig. 4 shows the spatial spectrum versus SNR, where the snapshots is fixed at 500, and the SNR varies from  $-10$  dB to  $10$  dB with  $2$  dB interval. Fig. 4(a) shows that when SNR equals to  $-10$  dB, classic MUSIC algorithm cannot recognize two closely placed signals. It can be seen from Fig. 4(b) that when SNR is at  $-10$  dB, the proposed algorithm can recognize two closely placed signals easily.

Fig. 5 shows the spatial spectrum versus snapshots, where the SNR is fixed at  $-10$  dB, the snapshots vary from  $100$  to  $1000$  with  $100$  intervals. From Fig. 5(a) and (b), we can see that when the snapshots equal to  $200$  and  $300$ , classic MUSIC cannot recognize two closely placed signals, while the proposed algorithm can easily distinguish them.

Fig. 6 shows the spatial spectrum versus sensor number, where the SNR and snapshots are fixed at  $-5$  dB and  $500$  respectively, the sensor number varies from  $8$  to  $20$  with  $2$  sensors interval. In Fig. 6(a), it can be seen that when sensor number equals to  $8$ , the MUSIC cannot recognize the two closely placed signals. In Fig. 6(b), it can be seen that if sensor number equals to  $8$ , the proposed algorithm can recognize the two closely placed signals. And when sensor number equals to  $10$ , the proposed algorithm can recognize the sources easily while MUSIC is difficult to recognize them.

Simulation results of Figs. 4–6 obviously demonstrate that the proposed algorithm has a higher resolution and higher spatial spectrum peaks compared with the MUSIC algorithm.

#### 4.3. Experiment 3: RMSE of the proposed and MUSIC algorithm

The root mean square errors (RMSE) is defined as

$$10\log_{10}\sqrt{\frac{1}{N}\sum_{n=1}^N\left[\frac{1}{P}\sum_{p=1}^P(\hat{\theta}_p(n)-\theta_p)^2\right]} \quad (\text{dB}) \quad (24)$$

where  $N = 1000$  represents the independent trials,  $P = 2$  represents the number of sources,  $\theta_p = (-3^\circ, 3^\circ)^T$  is the

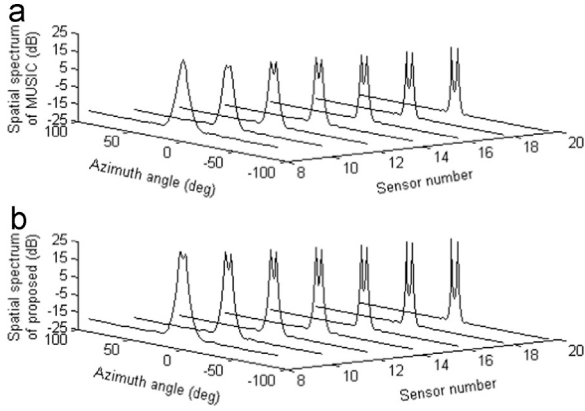


Fig. 6. Spatial spectrum versus sensor number.

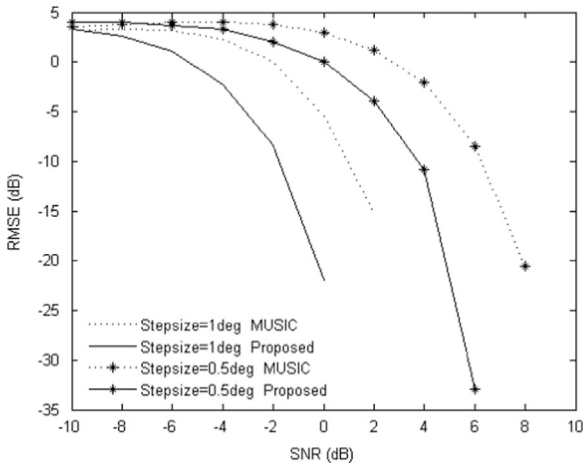


Fig. 7. RMSE versus SNR.

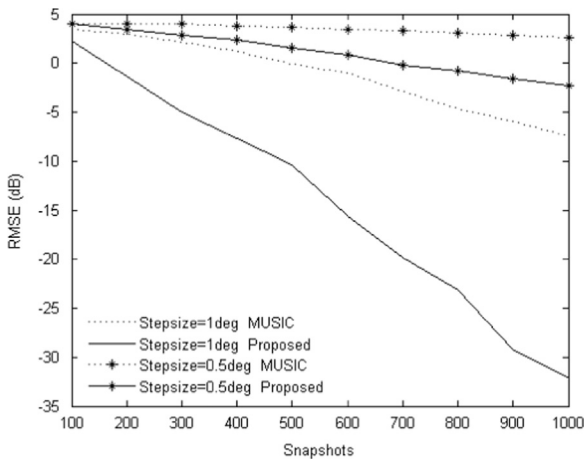


Fig. 8. RMSE versus snapshots.

azimuth angle of two impinging sources,  $\hat{\theta}_p(n)$  is the estimation of  $\theta_p$  for the  $n$ th Monte Carlo trial. According to the searching algorithm, we select the two azimuths corresponding to the first two highest peaks of spatial spectrum as  $\hat{\theta}_p(n)$ . The RMSE are presented in the cases of searching stepsize equal to  $0.5^\circ$  and  $1^\circ$ .

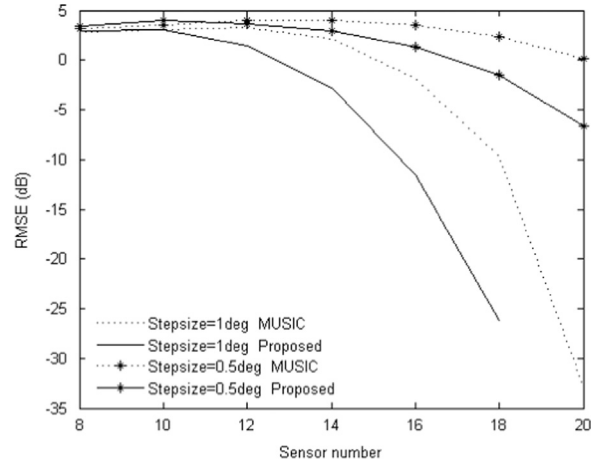


Fig. 9. RMSE versus sensor number.

Fig. 7 shows the RMSE versus SNR, where the snapshots is 200, the SNR varies from  $-10$  dB to  $10$  dB with  $2$  dB interval. Fig. 8 shows the RMSE versus snapshots, where the SNR is  $-5$  dB, and the snapshots vary from 100 to 1000 with 100 intervals. Fig. 9 shows the RMSE versus sensor number, where the SNR is  $-5$  dB, the snapshots are 200, and the sensor number varies from 8 to 20 with 2 interval. From Figs. 7 to 9, it can be seen that the improved MUSIC algorithm has better DOA estimation accuracy than classic MUSIC in each scenario.

## 5. Conclusions

In this paper, a cyclic optimization algorithm is proposed to calculate the signal subspace, the corresponding projection matrix of noise subspace is deduced, and an improved MUSIC algorithm is proposed. Experimental results show that the cyclic optimization algorithm can increase the accuracy of estimated signal subspace. The improved MUSIC algorithm has stronger ability to distinguish the closely set sources, and can obtain higher spatial spectrum peaks compared with the conventional MUSIC in the scenarios of SNR, snapshots and sensor number variation. The RMSE of estimated angles versus SNR, snapshots and sensor number are simulated, which shows an obvious accuracy improvement. It should be noted that the performance improvements of our algorithm is at the cost of computational consumption during the cyclic optimization procedure to obtain a high accuracy subspace.

## Acknowledgments

The authors would like to thank very much the Handling Editor Dr Ana Isabel Perez-Neira, Editor Chitra and the anonymous reviewers for their valuable comments and suggestions that have significantly improved the manuscript.

This work was supported by the National Natural Science Foundation of China under Grants 61373177 and

61271293; the Scientific Research Plan of Education Department of Shaanxi Province (11JK0903).

## Appendix A. Supplementary material

Supplementary data associated with this article can be found in the online version at <http://dx.doi.org/10.1016/j.sigpro.2015.12.002>.

## References

- [1] R.O. Schmidt, Multiple emitter location and signal parameter estimation, *IEEE Trans. Antennas Propag.* 34 (3) (1986) 276–280.
- [2] F. Wen, Q. Wan, R. Fan, et al., Improved MUSIC algorithm for multiple noncoherent subarrays, *IEEE Signal Process. Lett.* 21 (5) (2014) 527–530.
- [3] B.D. Rao, K.V.S. Hari, Performance analysis of ESPRIT and TAM in determining the direction of arrival of plane waves in noise, *IEEE Trans. Acoust. Speech Signal Process.* 40 (12) (1989) 1990–1995.
- [4] B. Ottersten, M. Viberg, T. Kailath, Performance analysis of the total least squares ESPRIT algorithm, *IEEE Trans. Signal Process.* 39 (5) (1991) 1122–1135.
- [5] B. Wang, Y.P. Zhao, J.J. Liu, Mixed-order MUSIC algorithm for localization of far-field and near-field sources, *IEEE Signal Process. Lett.* 20 (4) (2013) 311–314.
- [6] J.R. Magnus, H. Neudecker, *Matrix Differential Calculus With Applications in Statistics and Econometrics*, 2nd ed. Wiley, New York, 1991.
- [7] Y. Zhou, D.Z. Feng, J.Q. Liu, A novel algorithm for two-dimension frequency estimation, *Signal Process.* 87 (1) (2007) 1–12.
- [8] G. Dinolhac, P. Forster, F. Pascal, et al., Exploiting persymmetry for low-rank space time adaptive processing, *Signal Process.* 97 (2014) 242–251.
- [9] V.V. Reddy, B.P. Ng, A.W.H. Khong, Insight into MUSIC-like algorithm, *IEEE Trans. Signal Process.* 61 (10) (2013) 2551–2556.